



Heating a Large CTR Tokamak by Neutral Beam Injection

David G. McAlees and Robert W. Conn

December 1973

UWFDM-78

FUSION TECHNOLOGY INSTITUTE
UNIVERSITY OF WISCONSIN
MADISON WISCONSIN

Heating a Large CTR Tokamak by Neutral Beam Injection

David G. McAlees and Robert W. Conn

Fusion Technology Institute
University of Wisconsin
1500 Engineering Drive
Madison, WI 53706

<http://fti.neep.wisc.edu>

December 1973

UWFDM-78

Heating a Large CTR Tokamak by Neutral Beam Injection[†]

by

David G. McAlees*

and

Robert W. Conn

Nuclear Engineering Department
University of Wisconsin
Madison, Wisconsin 53706

December, 1973

(Submitted to Nuclear Fusion)

FDM 78

[†]Research supported by Wisconsin Electric Utilities Research Foundation and U.S.A.E.C.

*Present Address: Oak Ridge National Laboratory
Oak Ridge, Tenn. 37830

Heating a Large CTR Tokamak by Neutral Beam Injection

D. G. McAlees

R. W. Conn

Abstract

The startup of a large CTR Tokamak plasma at low density using energetic neutral beams is studied. Questions of beam energy deposition profiles, beam energy requirements for penetration, and beam power requirements to achieve ignition or prescribed plasma heatup rates are examined. A detailed analysis for a particular CTR system design, using a two fluid, space time numerical model to simulate plasma behavior is reported. The numerical model includes neoclassical ion conduction, pseudoclassical electron conduction, radiation losses, ohmic heating, thermonuclear alpha particle heating, and injection heating. It is found that even when the power density deposition profile for beam heating is peaked on axis, the plasma temperature profiles can have local maxima and thus be inverted in the outer plasma regions. This is caused by the decreased density in these zones. For a specific large system studied in detail (aspect ratio 2.6, plasma radius 500 cm, initial peak density $3 \times 10^{13}/\text{cm}^3$), beam energies of 100 KeV, 350 KeV, and 500 KeV are considered. Only the 500 KeV beam case yields non-inverted temperature profiles during heating. In all cases, moderate power levels are required to ignite low density plasmas in times on the order of seconds. In addition, the injection time required to establish a prescribed plasma heatup rate is examined in

detail. In some cases, for a given amount of injected energy, the heatup rate resulting from low energy beams is greater than that due to higher energy beams. Beam energy and power requirements for smaller systems are also given.

1. Introduction

The prospect of heating toroidally confined plasmas by energetic neutral beam injection has stimulated much interest and optimism in the beam heating technique and predictions for present day experiments⁽¹⁻⁴⁾ lend support to this optimism. Results have recently been reported from the ATC,⁽⁵⁾ CLEO,⁽⁶⁾ and ORMAK,⁽⁷⁾ experiments where modest amounts of power have been injected via neutral beams. Although the Tokamak injection experimental program is still at an early stage, these recent results indicate heating rates consistent with expectations with no apparent adverse effects on plasma confinement.

To assess the technological feasibility of developing large, power producing Tokamak systems, a number of groups have initiated design studies which focus on the system problems and requirements, in addition to the plasma physics problems. In this paper, the energy and power requirements for a neutral beam injection system capable of heating reactor size plasmas is examined.

The analysis is primarily for a 5000 MW(th) conceptual fusion reactor system, UWMAK-I, recently studied at the University of Wisconsin.⁽⁸⁾ However, the results are generally applicable to toroidal systems and, wherever possible, we have indicated the implications of our results for other, in particular, smaller feasibility or reactor size plasmas. The characteristics of the conceptual reactor, UWMAK-I, pertinent to this paper are listed in Table I and a more inclusive summary is given in Appendix A.

The plasma model and method of solution are discussed in Section 2. However, several general assumptions applicable to the model are the following: 1) the presence of background neutral gas and impurities in the plasma are not considered; 2) the possibility of a deleter-

ious plasma response due to neutral injection⁽⁹⁾ is not included;
 3) neoclassical ion transport and pseudoclassical electron transport^(15,16)
 are the only transport effects examined. Possible additional effects
 on transport, such as trapped particle instabilities⁽¹⁰⁾ are not studied.
 The remainder of the paper is structured as follows. In Section 3,
 we discuss the results obtained from the study of a particular large
 CTR Tokamak system. In Section 4, injection criteria are applied to
 a smaller system and the resulting beam energy and power requirements
 are discussed. The general conclusions of the analysis are summarized
 in Section 5.

2. The Calculational Model for Plasma Simulation

To simulate the time evolution of the plasma parameters during
 heating, a two-fluid numerical model, accounting for electromagnetic
 field diffusion and energy flows within the plasma, is used.⁽¹¹⁻¹³⁾
 The electron-ion fluid model accounts for diffusion, heat conduction,
 electron-ion rethermalization, bremsstrahlung and synchrotron radiation,
 ohmic heating, thermonuclear alpha particle heating and heating by
 means of injected power. The governing equations for the system are
 written in cylindrical coordinates and depend only on the minor radius,
 r , and the time, t . Toroidal transport coefficients, accurate to first
 order in $\epsilon = 1/A$, the inverse aspect ratio, are used. The equations
 are as follows:

1) Particle Conservation:

$$\frac{\partial n}{\partial t} = - \frac{1}{r} \frac{\partial}{\partial r} (r n W_r) + \frac{P(r)}{E_o} \quad (2.1)$$

where W_r is the radial diffusion velocity, $P(r)$ is the injected power density and E_o is the neutral beam particle energy.

2) Particle Diffusion:

$$n W_r = - D_{\perp} \frac{\partial n}{\partial r} \quad (2.2)$$

3) Ion Energy Conservation:

$$\begin{aligned} \frac{\partial}{\partial t} \left(\frac{3}{2} n T_i \right) = & 4.77 \times 10^{-12} \left(\frac{T_e - T_i}{T_e^{3/2}} \right) n^2 Z_i^2 \frac{\ln \Lambda}{A_i} \\ & - \frac{1}{r} \frac{\partial}{\partial r} \left(r \left\{ \frac{3}{2} n W_r T_i + Q_i \right\} \right) \\ & + \frac{n^2}{4} \langle \sigma v \rangle_{DT} E_{\alpha} f_{\alpha i} + P(r) f_{bi} \end{aligned} \quad (2.3)$$

$$Q_i = - \kappa_i \frac{\partial T_i}{\partial r} \quad (2.4)$$

where Q_i is the ion heat flux and f_{bi} is the fraction of beam power absorbed by the ions.

4) Electron Energy Conservation:

$$\frac{\partial}{\partial t} \left(\frac{3}{2} n T_e \right) = -4.77 \times 10^{-12} \frac{(T_e - T_i)}{T_e^{3/2}} \frac{n^2 Z_i^2 \ln \Lambda}{A_i}$$

$$\begin{aligned}
& - \frac{1}{r} \frac{\partial}{\partial r} \left(r \left[\frac{3}{2} n W_r T_e + Q_e \right] \right) + \frac{n^2}{4} \langle \sigma v \rangle_{DT} E_\alpha f_{\alpha e} + 6.25 \times 10^{14} E_\phi J_\phi \\
& + P(r) f_{be} - P_{Brem} - P_{sync}
\end{aligned} \tag{2.5}$$

$$Q_e = - \kappa_e \frac{\partial T_e}{\partial r} \tag{2.6}$$

$$P_{Brem} = 9.48 \times 10^{-17} Z_i^2 n^2 T_e^{1/2} \tag{2.7}$$

$$P_{sync} = 4.0 \times 10^{-12} B_\phi^{5/2} (1-R)^{1/2} n^{1/2} T_e^2 \tag{2.8}$$

Q_e is the electron heat flow, f_{be} is the fraction of beam energy absorbed by the electrons and R is the wall reflectivity to the synchrotron radiation. Eqns (2.2), (2.4), and (2.6) signify that a diagonal simulation model is being used. We do not include cross flow terms, such as energy flow due to density gradients or particle flows due to temperature gradients, which are expected on general grounds.⁽¹⁷⁾

P_{Brem} and P_{sync} represent energy losses from bremsstrahlung⁽¹⁸⁾ and synchrotron⁽¹⁹⁾ radiation, respectively.

The first term on the right hand side of eqns. (2.3) and (2.5) accounts for electron-ion rethermalization, and $P(r)f_{bi}$ and $P(r)f_{be}$ are external sources of energy for the ions and electrons, respectively. Also $E_\alpha = 3.5$ MeV is the energy of the alpha particle produced in a D-T fusion reaction, $f_{\alpha i}$ and $f_{\alpha e}$ are the fractions of the alpha energy deposited in the ions and electrons, respectively.⁽¹⁴⁾ The form of the particle and energy source terms due to neutral beam injection will be developed shortly.

5) Electromagnetic Equations:

$$\frac{\partial B_\theta}{\partial t} = 10^5 \frac{\partial E_\phi}{\partial r} \tag{2.9}$$

$$E_{\phi} = \eta J_{\phi} \quad (2.10)$$

In eqns (2.1) to (2.10), lengths are in cm, time is in milliseconds, density is in cm^{-3} temperature and energy are in eV, current density is in amps/cm^2 , electric fields are in Volts/cm, and magnetic field are in gauss.

Considerable theoretical work has been done in deriving transport theories for toroidal plasmas. It is still uncertain which theory describes present day experiments and whether or not direct scaling of any existing theory to large plasmas is appropriate. In this analysis, the electron heat conduction coefficient is assumed pseudoclassical^(15,16) and the ion heat conduction coefficient is taken as the banana regime of neoclassical theory.⁽¹⁷⁾ The particle diffusion coefficient, D_{\perp} , can be assumed zero for the large plasmas studied in this paper. This simplification is justified by estimating the particle confinement time as $\tau_p \approx \frac{a^2}{4D_{\perp}}$. Based on the initial plasma conditions and taking D to be pseudoclassical, typical particle confinement times are found to be greater than 50 seconds. The time scale for heating the plasma is expected to be on the order of 10 seconds or less so that particle diffusion during the heating phase is negligible. The plasma density profile thus changes during heating only as a result of the addition of plasma particles by neutral injection. The transport coefficients used in the numerical simulation are given by,

$$\kappa_i = 0.68 \epsilon^{1/2} \rho_{i\theta}^2 n v_i \quad (2.11)$$

$$\kappa_e = 10 n v_e \rho_{e\theta}^2 \quad (2.12)$$

$$D_{\perp} \approx 0. \quad (2.13)$$

The forms of bremsstrahlung and synchrotron radiation loss terms and the electrical resistivity are those of Rose and Clark⁽¹⁸⁾, Rosenbluth⁽¹⁹⁾, and Spitzer⁽²⁰⁾, respectively. A reflection coefficient of 0.9 is assumed in the case of synchrotron radiation.

Equations (2.3) and (2.5) include terms representing the energy deposited in the plasma by alpha particles produced in deuterium-tritium fusion events. We assume that the flux surfaces in the plasma are circular and that an alpha particle deposits 3.5 MeV uniformly over the flux surface on which it is produced. In addition, the characteristic slowing down time for an alpha particle in an electron density of 3×10^{13} electrons/cm³ at a temperature of 5 KeV is less than half a second. Therefore, it is assumed that the alpha particle energy is instantaneously deposited in the plasma.

The equations for the model are non-linear coupled differential equations and require linearization of the transport coefficients. Following linearization, an implicit finite difference method⁽²¹⁾ is used to obtain the time dependent radial profiles. Details of the numerical solution method are given by Dory and Widner.⁽¹²⁾

The neutral beam heating phase of reactor startup is assumed to follow initial gas breakdown and the time during which the plasma current rises to its final operating value. During the beam heating phase, the plasma current remains fixed and the core flux is increased to make up for the resistive drop as the plasma temperature increases. Thus, the times to ignition given in the next section refer strictly to the beam heating phase and do not include the current rise time.

(The current rise time in Tokamak reactors may be long because of the large energy stored in the fields of the transformer and divertor coils.⁽⁸⁾)

The analysis here begins with a fully ionized plasma characterized by the following relatively flat radial dependent profiles:

$$T_i(r,t=0) = T_{i0}(1 - r^2/a^2)^{1/3} + 10\text{eV}, \quad T_{i0} = 500 \text{ eV} \quad (2.14)$$

$$T_e(r,t=0) = T_{e0}(1 - r^2/a^2)^{1/3} + 10\text{eV}, \quad T_{e0} = 500 \text{ eV} \quad (2.15)$$

$$n(r,t=0) = n_0(1 - .95 r^2/a^2)^{1/2}, \quad n_0 = 3 \times 10^{13}/\text{cm}^3 \quad (2.16)$$

$$J_\phi(r,t=0) = J_0(1 - r^2/a^2)^{1/2}, \quad J_0 = 40.2 \text{ amps/cm}^2 \quad (2.17)$$

$$E_\phi(r,t=0) = \eta J_\phi(r,t=0) \quad (2.18)$$

The initial temperature profiles are assumed relatively flat because the conceptual reactor, UWMAK-I, is proposed to operate with an axisymmetric, poloidal field divertor. The action of the divertor should mean that a relatively rarefied zone, dominated by atomic processes, will surround the plasma outside the separatrix. The 10 eV temperature is inserted to indicate the presence of this blanket plasma. The density profile given by equation (2.16) is also relatively flat and the factor, .95, means the density on the edge will be roughly 20% of the center line density. We have varied the boundary temperature from 10 eV to 100 eV and varied both the shape of the density profiles and the density of the plasma at the edge. It is found that the plasma heat up rates are basically not affected. On the other hand, beam penetration is strongly dependent on the density profile. Actual beam power deposition profiles for different density

profiles will be given shortly. Finally, the safety factor, $q(a)$, is set at 1.75 and the initial profiles are consistent with $q > 1$ at all plasma radii.

The energetic neutral beam injected into plasma is assumed to be composed of a deuterium-tritium neutral of atomic mass 2.5. A single equivalent atom beam of zero cross sectional area (pencil beam) is considered. In practice, the required total power would be injected by several neutral beams located symmetrically around the torus to minimize the disturbance of axisymmetry in the plasma. Rome, Callen and Clarke⁽²²⁾ have recently studied the injected energy density deposition rate profiles which result from finite beams. We find, using the computer code developed in their work, that the pencil beam approximation is accurate except in the region near the plasma center. For the system studied in Section 3, the pencil beam and finite beam give essentially the same results for $r \gtrsim .15a$. In addition, the time required to heat the plasma to ignition is not sensitive to the detailed injected energy profile near $r = 0$ since the toroidal plasma volumes in this region are small.

The neutral beam strength is defined, in equivalent amperes, by

$$I = P_T/E_0 \quad (2.19)$$

where P_T is the beam power in watts and E_0 is the beam particle energy in electron volts. The number of particles injected into the plasma per second, I/e , where e is the electron charge, is accounted for in equation (2.1).

The neutral beam particles are ionized in the plasma primarily by electron and ion impact and by charge exchange.⁽²³⁾ The optimum choice for the angle of injection is not clear. However, injection nearly perpendicular to the toroidal field will result in fast ion production trapped particle orbits. This trapped ion specie may support trapped particle instabilities and a distributed charge distribution⁽⁹⁾ in the plasma which could cause plasma rotation. Therefore, we have chosen to analyse tangential injection. The geometry for neutral beam injection tangent to the center of the cross section is shown in Figure 1. For a neutral current, I_0 , entering the plasma, the attenuation of the beam as a function of distance along the injection chord is given by,

$$I(s) = I_0 e^{-\int_0^s n(s') \sigma_T ds'} \quad (2.20)$$

where

$$\sigma_T = \sigma_{cx} + \sigma_i + \frac{\langle \sigma v \rangle}{v_0} \quad (2.21)$$

σ_{cx} is the charge exchange cross section, σ_i is the ion impact cross section, $\frac{\langle \sigma v \rangle}{v_0}$ is the Maxwellian averaged electron impact cross section, v_0 is the neutral particle velocity and s is the distance along the chord. It is assumed that the cross sections are functions of the relative velocity of the colliding species only. For the beam energies examined in this paper ($E_0 > 100$ KeV), ion and electron impact ionization are dominant and charge exchange is small. Thus, neutral injection is not a source of warm neutrals as it can be in present injection experiments. Numerical values of the cross sections are given in references (23) and (24). We use the approximation to the data given by Sweetman⁽²⁵⁾ and shown in Figure 2. In the worst case, equivalent to a 200 KeV hydrogen neutral, the error introduced by this fit to the attenuation cross section is 25%.

The drift orbits of the fast ions produced as the neutrals are ionized must be considered in determining the energy density deposition rate in the plasma. It has been shown that ions produced parallel to the magnetic field follow orbits which are approximately circular and centered at $x = x_s$, when projected onto a plane containing the plasma cross section. (1,22) The stagnation distance, x_s , is defined by

$$x_s \doteq qmv_{\phi}/eB_{\phi} \quad (2.22)$$

and for 500 KeV injected ions, the center of the orbit is $x_s \approx 7$ cm in a system the size of UWMAK-I. Since x_s is less than 7 cm for injection energies less than 500 KeV, this small shift in the orbit center is neglected. Thus, the fast ions resulting from injection are assumed to traverse circular orbits centered at $r=0$.

The fast ion slowing down time, as for the alpha particles, is short compared with the particle confinement time so that it is assumed the ions deposit energy instantaneously over the flux surface on which they are produced. The radial shape of the energy density deposition rate for a particular beam energy is calculated numerically using the attenuation and orbit considerations just outlined and the assumed plasma density profile. In addition, the total beam power has a radial distribution in the plasma. Therefore, the total power deposited is defined as

$$P_T = 2\pi R_o \int_0^a 2\pi r P_o f(r) dr, \quad (2.23)$$

where $P(r) = P_0 f(r)$ is the energy density deposition rate profile, P_0 is the power density at $r=0$, and $f(r)$ is the radial shape factor for a beam of energy E_0 . The shape factor $f(r)$ is calculated numerically and is included in equations (2.3) and (2.5) in this manner.

In a large plasma governed by the transport laws we have assumed, the time scale for rethermalization between plasma electrons and ions is small compared to the plasma heating time. Therefore, the heating times calculated are not sensitive to the exact fraction of the injection energy absorbed by each plasma specie as the fast ion slows down. We have assumed 70 percent of the injected energy is absorbed by the electrons in all cases considered in Sections 3 & 4.

3. Plasma Heating by Neutral Beam Injection

The characteristics of a reactor size plasma studied here are given in Appendix A and pertinent parameters are listed in Table I for convenient reference. The approach of the plasma toward thermal equilibrium, considering only ohmic heating and no beam heating, has been calculated for a five second time interval. The peak ion temperature as a function of time is given on Fig. 3. Using the Spitzer formula for electrical resistivity,⁽²⁰⁾ ohmic heating alone is not sufficient to ignite the system. Using the notation, $T(r,t)$, one notes that $T_i(0,\infty)$ is less than 3 KeV. Further, since the temperature rise due to ohmic heating is a relatively slow process, there is no advantage in delaying injection heating until the ohmic heating phase has concluded. Therefore, injection heating will begin immediately after the plasma current has been fully established, i.e., $t=0$ with respect to the heating phase.

We now consider the neutral beam energy and power that are required to ignite such a reactor size plasma. Clearly, the beam must be energetic enough to adequately penetrate the plasma before ionization occurs. On the other hand, the beam energy is bounded from above by requiring that a large fraction of the injected neutral particles be trapped in the plasma. In large systems, such as UWMAK-I, this maximum energy requirement is really inconsequential since trapping of the injected neutrals is highly efficient.

Since the plasma is quite large in this system, we have chosen to ignite the plasma at low density, $n_0 = 3 \times 10^{13} / \text{cm}^3$, to improve beam penetration. We assume subsequent fueling after ignition can build the plasma density to a desired operating value. In addition to the penetration problem, the stored energy in the hot, dense operating plasma is very high, on the order of 1000 MJ. Therefore, it is advantageous to ignite the system at a lower stored energy. Stix⁽¹⁾ and Girard, Khallidi, and Marty⁽²⁶⁾ have come to the same conclusion based on similar considerations. By heating the plasma to a temperature above the ignition temperature, the stored energy will increase further due to thermonuclear power, and fueling can then be accomplished by alternate means.⁽²⁷⁾

The radial shapes of the power density deposited in the plasma from 100, 350, and 500 KeV beams are shown on Fig. 4. The shape factors are independent of the total power in the beams and are normalized to 1.0 at the radius of maximum deposition. the fraction of the 100, 350, 500 KeV beams trapped in the plasma are >.999, >.999, and >.995, respectively. The effect of different density profiles for the 350 KeV beam is shown in Fig. 5. It is clear that the most concave density profile gives the most peaked power deposition profile. However we have found that the plasma heating rate and the time to ignition are only slightly affected.

Since we consider plasma heating at a density below that desired during the burn, we are interested in both igniting the plasma and perhaps more importantly, in achieving a prescribed heatup rate to allow for subsequent fueling and density buildup. A rigorous monitor of plasma behavior relevant to ignition and heatup is the plasma stored energy, W , defined as

$$W(t) = \int_0^t (P_{\alpha} + P_{OH} + P_{INJ} - P_L) dt' \quad (3.1)$$

Here, P_{α} , P_{OH} , and P_{INJ} are the powers due to alpha particles, ohmic heating and injection, respectively, and P_L is the total power loss from the plasma volume. The rate of change of the stored energy is

$$\frac{dW(t)}{dt} = P_{\alpha} + P_{OH} + P_{INJ} - P_L \quad (3.2)$$

From eqn. (3.2), one sees of course that W will increase without injection if

$$P_{\alpha} + P_{OH} > P_L \quad (3.3)$$

This condition, $P_{\alpha} + P_{OH} = P_L$, can occur at low temperature when the plasma approaches a thermal equilibrium maintained by ohmic heating. It also occurs at a higher temperature when the power deposition from alpha heating becomes dominant and the plasma ignites. As the plasma approaches the lower temperature equilibrium, the stored energy is increasing but dW/dt is decreasing and d^2W/dt^2 is negative. This equilibrium point is thermally stable, i.e., stable against excursions in plasma temperature. On the other hand, if beam heating is used until

d^2W/dt^2 becomes positive, the plasma will have reached the higher temperature, thermally unstable, ignition point and the plasma will have ignited. (If plasma resistivity is anomalously large, ohmic heating alone could drive d^2W/dt^2 positive and the plasma will ignite without auxiliary heating.) Once d^2W/dt^2 is positive, the plasma will have a positive heatup rate even if beam heating is discontinued.

The reason is the second derivative,

$$\frac{d^2W}{dt^2} = \frac{d}{dT} (P_{\Omega} + P_{\alpha} - P_L) \frac{dT}{dt}, \quad (3.4)$$

can be positive only when P_{α} is dominant since $\frac{d}{dT} (P_{\Omega} - P_L)$ is negative and $\frac{dT}{dt}$ is positive. Therefore, assuming constant injection power, the ignition condition is

$$\frac{d^2W}{dt^2} > 0. \quad (3.5)$$

At the time of ignition, injection can be discontinued and the plasma will heatup at an accelerating rate.

Fig. 6 illustrates these points by showing the heating rates resulting from 75 MW of injection for 5 seconds and for three different beam energies. In all cases, the plasma is ignited in less than 5 seconds. Ignition occurs where dW/dt is a minimum. When the beams are turned off at $t = 5$ sec, the 500 KeV case exhibits the fastest heatup rate, approximately 7.5 MJ/sec. However, the 100 KeV beam has been more efficient in heating the plasma than the 350 KeV beam. When the beams are turned off, the 100 KeV case gives a heating rate of 5.9 MJ/sec compared to 2.3 MJ/sec from the 350 KeV beams. The reasons for this difference can be understood by examining the ion temperature profiles in Figures 7, 8, and 9.

One notes first that injection of 500 KeV beams for 5 seconds produces high ion temperatures in the central zone of the plasma. Therefore, the production rate of alpha particles is also high in this zone and the result is an appreciable total alpha power production. In the 100 KeV case, the maximum ion temperatures are lower and occur near the plasma edge. However, the plasma volume associated with the high temperature zone is greater than for the 500 KeV beam case. As such, the total alpha power produced is again appreciable. The 350 KeV neutral beam is calculated to produce a relatively uniform ion temperature profile. However, the temperature level of approximately 6 KeV means the total alpha power produced is, in fact, less than in each of the previous two cases. The result is the low heatup rate of 2.3 MJ/sec once injection is terminated. We conclude that the plasma heatup rate resulting from injection at constant power for a specific length of time depends on the ion temperature profiles established in the plasma. This in turn is clearly a function of the beam energy.

Turning to another point, Figure 10 illustrates the effects of using different beam powers at a given beam energy. The calculations were for 10 seconds of neutral beam injection in both cases. For 25 MW of 500 KeV beams, the plasma barely ignites and d^2W/dt^2 is positive but small. The heatup rate is thus also small. On the other hand, 50 MW of power produces a heatup rate of approximately 24 MJ/sec. This can be compared to the 75 MW, 500 KeV, 5 second injection case shown in Fig. 6 where the heatup rate at the end of injection is 6.8 MJ/sec. A cross comparison of Figures 6 and 10 indicates, for various

beam energies and different beam powers, the time required to ignite the plasma and the heatup rates which result from injection times in the 5 to 10 second range.

Some further comments should be made on the temperature profiles shown in Figures 7, 8, and 9. In the 100 KeV case shown on Fig. 7, the beam energy is too low to penetrate the plasma appreciably. The injected power is therefore deposited in the outer plasma regions. Yet even with the steep temperature gradients that develop, energy transport from large to small plasma radii is too slow to cause appreciable temperature increase at the plasma center. The implication is that for large plasmas operating at low q values, and governed by the transport coefficients we have assumed, the plasma energy balance is local. That is, two adjacent volumes of plasma are only weakly coupled energetically. As such, the plasma temperature profile can be expected to follow the injected power profile.

The strongly inverted temperature profiles in the 100 KeV beam case are similar to profiles predicted to develop from skin currents and may have adverse effects on plasma confinement. The questions of plasma equilibrium and stability are not investigated here. Rather, we have determined the beam energy necessary to produce non-inverted temperature profiles. The injection profile for a 350 KeV beam does not have a local peak off axis, as is seen in Fig. 4, case (b). The temperature response to a 75 MW, 350 KeV neutral beam has been computed and the profiles are given in Fig. 8. As with the 100 KeV beam, though to a lesser extent, the temperature profiles are locally peaked off axis even though the injected energy density deposition rate is maximum on axis and is monotonically decreasing to $r=a$. This result

is clarified by considering Fig. 11.

Fig. 11 shows the 350 KeV injection case, renormalized on a power deposited per plasma particle basis. Since the plasma density decreases monotonically with radius, the 350 KeV beam produces a heating rate (as opposed to an energy density deposition rate) which is a maximum on axis but is also locally peaked near the plasma boundary. Therefore, even a constant power density input can result in preferential heating off axis because the plasma density decreases with radius.

A 500 KeV beam does yield plasma temperature profiles in this reactor size plasma that are not inverted. Yet this energy is less than the approximately 1 MeV beams previously suggested to achieve adequate penetration in a somewhat smaller toroidal plasma.⁽²³⁾ We find that a lower beam energy is acceptable for three reasons; 1) a low density startup is used, ($3 \times 10^{13} \text{ cm}^{-3}$ vs $3 \times 10^{14} \text{ cm}^{-3}$ in reference (23)), 2) the density profile is included in the calculation, and 3) the variation with radius of the plasma volume per radial increment along the tangential injection path shown in Fig. 1 is included. The temperature response to 75 MW of 500 KeV beam particles is shown in Fig. 9. Again, we discontinued injection heating in the calculations after 5 seconds.

The use of 75 MW of neutral beam power gives examples of fast plasma heating and thus rapid startups. Since the burn time for reactors may be long, (approximately 2000 seconds for the reactor studied in reference 8), a slower startup is acceptable. A slower startup may be desirable since there is a trade-off between the time to ignition and the power required. Fig. 12 shows the power required for igni-

tion as a function of the time to ignition, using 500 KeV beams. Even a long startup (for example, the 15 MW case) requires only about 10 seconds. Depending on the additional time required to increase the density and temperature to operating conditions after ignition, the time for ignition can be shortened by increasing the beam power.

4. Impact of Results on Other Machines

This work has concentrated on the neutral beam heating of the large, power producing conceptual CTR Tokamak system outlined in Appendix A. Further, we have indicated the reasons that the neutral beam energy and power required to ignite the plasma depend directly on the detailed plasma characteristics and profile shapes. To determine how these results scale with system size, we have analyzed a system with a plasma radius of 2 meters, a major radius of 5.2 meters and otherwise identical to the conceptual design, UWMAK-I, in toroidal field strength, MHD safety factor, profile shapes, and so on. To obtain the same injected power deposition profile as in the 500 KeV case studied in section 3, one must keep a/λ_0 the same in both cases. a/λ_0 is the ratio of plasma radius to the mean free path of the injected neutrals at the peak plasma density (see Fig. 2). The required beam energy in the 2 meter system is approximately 200 KeV. Fig. 13 shows the power required to ignite this smaller system, as a function of the time to ignition, using a 200 KeV neutral beam. In both the case of UWMAK-I and the system with a 2 meter plasma radius, the beam energy required may be reduced in two ways. First, we have assumed for calculational convenience that the injected neutral has an atomic mass of 2.5. The total attenuation cross section for the neutral beam

is a function of the relative velocity of the beam particles and the background plasma. For the same relative velocity, the beam energy required varies linearly with mass. Therefore, the minimum energy required is reduced by 20 percent if a pure deuterium neutral beam is used. Second, as pointed out in reference (22), the beam can be injected inside the geometric center of the plasma cross section, which results in a shorter chord length to the plasma center. Changing the injection angle requires consideration of the finite size of the beam to be certain the beam does not intersect the torus inner wall. Also, additional analysis of the orbits of ions produced at large pitch angles is required.

5. Conclusions

The analysis reported in the preceeding sections, based on pseudoclassical scaling for the electron conductivity and neoclassical scaling for the ion conductivity, indicates that large Tokamak plasmas can be ignited at low density ($\sim 3 \times 10^{13}$ particles/cm³) using moderate levels of neutral beam power and beam energies of several hundred KeV. For a reactor size plasma with a minor radius of 5 meters and characteristic parameters as listed in Table I, a 500 KeV beam is adequate to provide the injected power deposition and heating rate profiles that ignite the plasma and yield non-inverted temperature profiles. Lower beam energies can also yield injected power deposition profiles that are peaked on axis. However, the heating rate in the plasma causes local maxima to occur in the temperature profiles in the outer zones of the plasma. This is found in the analysis of smaller systems as well. The maxima develop because the injected power deposited per

plasma particle depends on the density profile. For a scaled down machine with $a=200$ cm and the same aspect ratio, 200 KeV gives results similar to the 500 KeV beam in the larger system.

A low density startup is used because beam penetration is enhanced while plasma losses are reduced. Therefore, a large system can be ignited in reasonably short times. For example, in the conceptual UWMAK-I system studied here, power levels on the order of 50 MW give ignition times in the 2 to 10 second range. In smaller feasibility or reactor size plasmas, such as the $a=200$ cm system, approximately 10 MW of beam power is sufficient to ignite the system in about 2 seconds with 200 KeV beams.

The time to ignite reactor size plasmas using a given beam power are found to be about the same where beam energies are in the range from 100 KeV to 500 KeV ($A_1 = 2.5$). However, the final heatup rate of the plasma is sensitive to beam energy when a given power is injected for a fixed length of time. In particular, we have found that lower energy, less penetrating, neutral beams can actually produce faster plasma heating rates in some cases.

Finally, we note that the time scale for heat conduction using pseudoclassical and/or neoclassical transport coefficients is long in a large plasma compared with the heating times of several seconds. As such, thermal diffusion does not effectively suppress the local maxima in the temperature profiles which are reported here. For the same reason, adjacent volumes of plasma are found to be very weakly coupled, from an energy viewpoint, so that approximately equal electron and ion temperatures are found throughout the beam heating phase.

Appendix A

Characteristics of UWMAK-I

We list in this appendix a more inclusive, though by no means complete, set of parameters characterizing the UWMAK-I conceptual Tokamak fusion reactor recently studied at the University of Wisconsin.⁽⁸⁾ In particular, the discussion is limited primarily to those parameters that describe the plasma and magnets.

The primary operating characteristics of UWMAK-I are:

Power	5000 MW(th); 1500 MW(e)
Fuel Cycle	(D-T), Li
Plasma Radius	5 m
Major Radius	13 m
Divertor	Poloidal, Double Neutral Point
Coolant	Lithium
Structural Material	316 Stainless Steel
Neutron Wall Loading	1.25 MW/m ²
Toroidal Magnetic Field	$B_T = 38.2$ KGauss on axis $B_T^{\max} = 86.6$ KGauss at magnet
Magnets	Superconductor, NbTi Stabilizer, Cu
Power Cycle	Li-Steam

The main plasma characteristics which describe UWMAK-I during the beam heating phase of startup are:

$$\text{Peak plasma density: } 3 \times 10^{13}/\text{cm}^3$$

$$\text{Safety factor: } q(a) = \frac{a}{R} \frac{B_\phi}{B_\theta(a)} = 1.75$$

$$q(o) > 1$$

Plasma Current	$I_p = 21 \times 10^6 \text{ amps}$
----------------	-------------------------------------

The plasma characteristics which describe UWMAK-I during the operating phase are:

Poloidal Beta	$\beta_\theta = 1.08$
Toroidal Beta	$\beta_\phi = 0.052$
Safety Factor	$q(a) = 1.75; q(o) > 1$
Toroidal Magnetic Field	38.2 KGauss on axis
Plasma Current	$21 \times 10^6 \text{ amps}$
Ion Temperature	11 KeV
Electron Temperature	11 KeV
(D+T) Ion Density	$0.8 \times 10^{14} / \text{cm}^3$
Alpha Density	$0.03 \times 10^{14} / \text{cm}^3$
Particle Confinement Time	14 seconds
Fractional Burnup	7.2%

$$\langle Z_{\text{eff}} \rangle = \sum_j \frac{n_j Z_j^2}{n_e} = 3.3$$

Burn Time	90 minutes
-----------	------------

UWMAK-I is designed to operate with a poloidal, double-neutral point divertor which produces a low density, essentially insulating zone, around the plasma. As such, the temperature profile during the burn time is expected to be relatively flat, whereas the density profile has been assumed to have the shape, $n(r) = n_o (1 - .99 r^2/a^2)^{1/2}$.

Further design details are given in reference 8.

Acknowledgment

The authors thank Drs. J. D. Callen, J. T. Hogan, J. A. Rome, and C. W. Maynard for discussions and the Oak Ridge National Laboratory for use of their computing facilities. This research was supported by the Wisconsin Electric Utilities Research Foundation and the U.S.A.E.C.

References

1. T. H. Stix, Plasma Physics 14, (1972) 367.
2. R. Dei-Cas, et al, "The Neutral Injection Heating into the Fontenay-Aux-Roses Tokamak," Paper E9, Third Intl. Symposium on Toroidal Plasma Confinement, Max-Planck-Institut fur Plasma Physik, Garching (1973).
3. L. D. Stewart, et al., "Neutral Beam Injection Heating of ORMAK," Paper E12, Third Intl. Symposium on Toroidal Plasma Confinement, Max-Planck-Institut fur Plasma Physik, Garching (1973).
4. D. Aldcroft et al, Nuclear Fusion 13, (1973) 393.
5. K. Bol et al, Proc. Sixth European Conf. on Controlled Fusion and Plasma Physics, Moscow, (1973) Vol. II (to be published).
6. J. Sheffield et al, Ibid.
7. C. F. Barnett et al, Ibid.
8. B. Badger et al, "Wisconsin Tokamak Reactor Design UWMAK-I," (University of Wisconsin Fusion Design Memo 68, Nucl. Eng. Dept., University of Wisconsin, Madison, November 1973) Vol. I.
9. J. D. Callen et al, "Theory of Neutral Beam Injection into a Tokamak," Paper E14, Third Intl. Symposium on Toroidal Plasma Confinement, Max-Planck-Institut fur Plasma Physik, Garching (1973).
10. B. B. Kadomtsev and O. P. Pogutse, Nuclear Fusion 11, (1971) 67.
11. The computer simulation model used herein was developed from the model discussed in references 12 and 13.
12. R. A. Dory and M. M. Widner, Bull. Am. Phys. Soc. 11, (1970) 1418, Also ORNL-TM-3498.
13. J. T. Hogan and R. A. Dory, Proc. Fifth European Conf. on Controlled Fusion, Grenoble (1972) Vol. I, p. 40.
14. D. J. Sigmar and G. Joyce, Nuclear Fusion 11, (1971) 447.
15. S. Yoshikawa, Phys. Fluids 13, (1970) 2300.
16. L. A. Artsimovich, Soviet Physics JETP Letters, 13, (1971) 70.

17. M. N. Rosenbluth, R. D. Hazeltine and F. L. Hinton, Phys. Fluids 15, (1972) 116.
18. D. J. Rose and M. Clark, Jr., Plasmas and Controlled Fusion, (2nd revised printing, M.I.T. Press, Cambridge, Mass. 1965).
19. M. N. Rosenbluth, Nuclear Fusion 10, (1970) 340.
20. L. Spitzer, Jr., Physics of Fully Ionized Gases, (2nd revised edition, Interscience Publishers, New York 1967).
21. R. D. Richtmyer and K. W. Morton, Different Methods for Initial Value Problems, (2nd revised edition, Interscience Publishers, New York, 1967).
22. J. A. Rome, J. D. Callen and J. F. Clarke, "Neutral Beam Injection in a Tokamak I: Fast Ion Spatial Distribution for Tangential Injection" (to be published). (Also, Oak Ridge Nat'l Lab., Report ORML-TM-4332 (1973).
23. A. C. Rivere, Nuclear Fusion 13, (1971) 367.
24. W. Lotz, Astrophys. Journ, Suppl. No. 129, XIV (1967) 207.
25. D. R. Sweetman, Nuclear Fusion 13, (1973) 157.
26. J. P. Girard, M. Khelladi, and D. A. Marty, Nucl. Fusion 13, (1973) 685.
27. For example, using pellet injection to increase the density to a desired operating value. See S. L. Gralnick, Nucl. Fusion 13, (1973).

Figure Captions

1. (a) Geometry for neutral injection tangent to the geometric center of the plasma. (b) Plasma cross section view showing a typical fast ion orbit.
2. Mean free path and reciprocal of the total attenuation cross section for injected neutrals, as a function of the neutral particle energy, using the fit giving by Sweetman.⁽²⁴⁾ (λ_o evaluated at a density of $3 \times 10^{13}/\text{cm}^3$.)
3. Peak ion temperatures as a function of time for the ohmically heated case. There is no neutral beam energy injected.
4. Radial shape factors for beam energies of 100, 350, and 500 KeV. Shape factors are normalized to 1.0 at the radius of maximum deposition.
5. Radial shape factors for a 350 KeV beam injected into a plasma with different density profiles.
6. Heatup rate as a function of time for 75 MW of power injected at 100, 350, and 500 KeV for 5 seconds.
7. Radial ion temperature profiles after 1, 5, and 10 seconds resulting from injection of 75 MW of 100 KeV neutrals for 5 seconds.
8. Radial ion temperature profiles after 1, 5, and 10 seconds resulting from injection of 75 MW of 350 KeV neutrals for 5 seconds.
9. Radial ion temperature profiles after 1, 5, and 10 seconds resulting from injection of 75 MW of 500 KeV neutrals for seconds.
10. Heatup rate as a function of time for 25 and 50 MW of power at 500 KeV injected for 10 seconds.
11. Radial profile of the power density deposited per plasma particle by a 350 KeV beam.
12. Power for ignition as a function of time to ignition ($a=5\text{m}$) using 500 KeV beams.
13. Power required to achieve ignition as a function of time to ignition in a 2m plasma ($A=2.6$) using a 200 KeV beam.

Table I

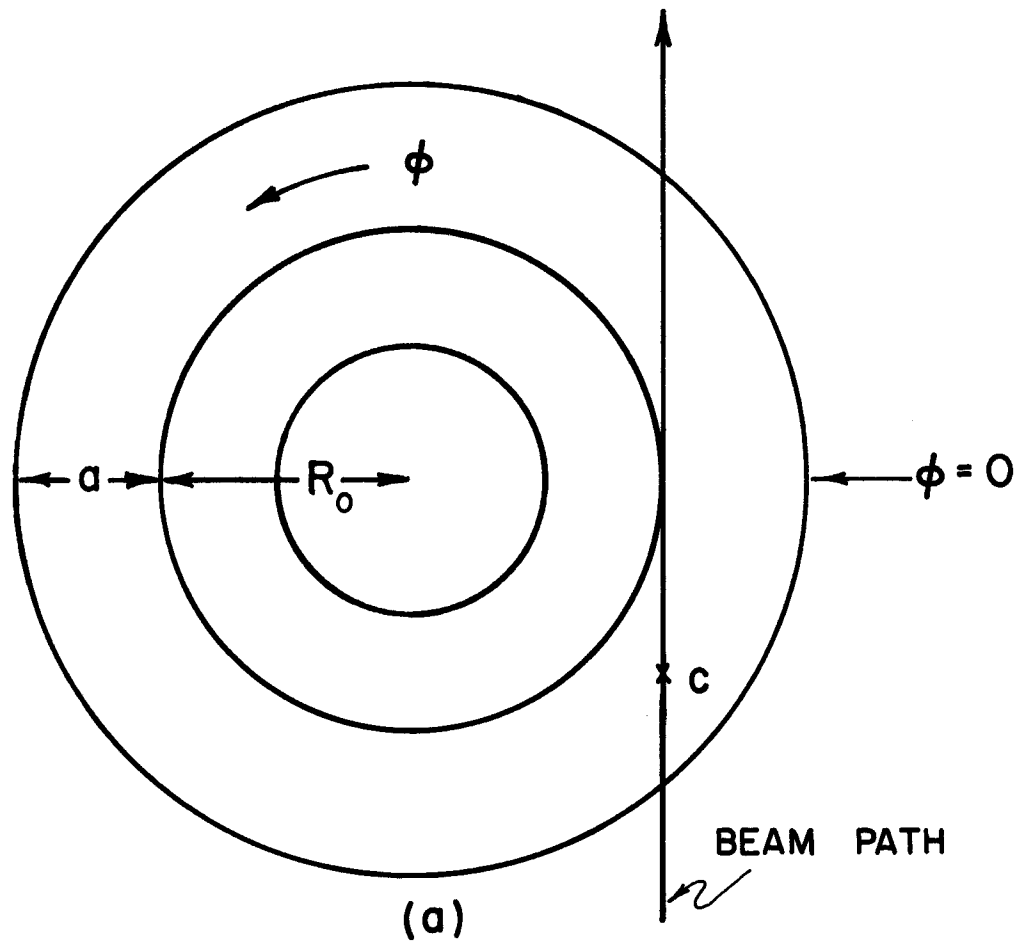
Relevant Characteristics of UWMAK-I,
A Conceptual CTR Tokamak Power Reactor⁽⁸⁾

Plasma Radius	5	m.
Major Radius	13	m.
Toroidal Field on Axis	38.2	KGauss
Poloidal Beta, β_θ	1.08	
Toroidal Beta, β_ϕ	0.052	
Safety Factor, $q(a)$	1.75	
Plasma Current	21	MAmps
Burn Time	5400	sec.

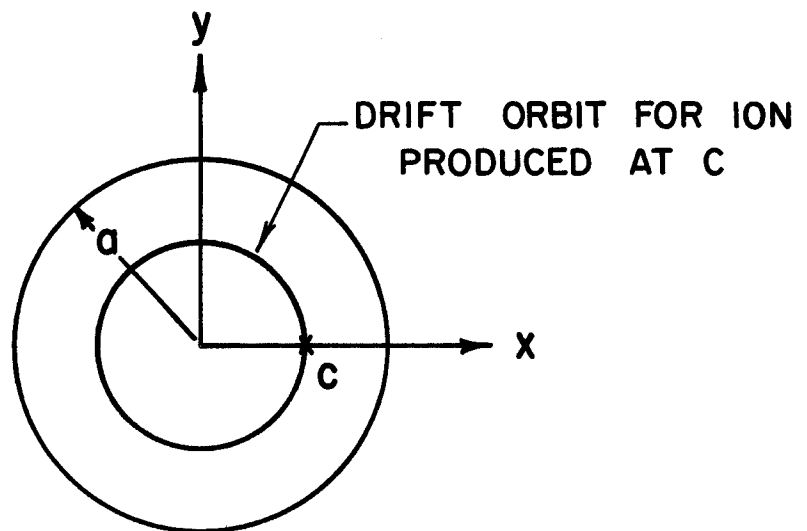
TABLE 1

RELEVANT CHARACTERISTICS OF UWMAK-I,
A CONCEPTUAL CTR TOKAMAK POWER REACTOR

PLASMA RADIUS	5 m.
MAJOR RADIUS	13 m.
TOROIDAL FIELD ON AXIS	38.2 KGauss
POLOIDAL BETA, β_{θ}	1.0
TOROIDAL BETA, β_{ϕ}	0.05
SAFETY FACTOR, $q(a)$	1.75
PLASMA CURRENT	21 MAmps
BURN TIME	2100 sec.



(a)
TOP VIEW OF PLASMA



(b)
CROSS SECTION VIEW OF PLASMA

